
Article:
Owen, Joseph, Pasley, John Richard orcid.org/0000-0001-5832-8285 and Ridgers, Christopher Paul orcid.org/0000-0002-4078-0887 (2021) Investigation of the performance of mid-Z hohlraum wall liners for producing X-ray drive. Physics of Plasmas. 012703. ISSN 1089-7674

https://doi.org/10.1063/5.0029689

Investigation of the performance of mid-Z hohlraum wall liners for producing X-ray drive

J. Owen,* J. Pasley, and C. P. Ridgers
York Plasma Institute, University of York, Heslington, York YO10 5DQ, United Kingdom

M-band transitions (n = 4 → 3) in Gold are responsible for a population of X-rays with energy > 1.8 keV in indirect drive inertial fusion. These X-rays can preheat the fuel, cause the ablator-fuel interface to become unstable to Rayleigh-Taylor instabilities, and introduce radiation non-uniformity to the X-ray drive. This work investigates the performance of mid-Z lined hohlraums for producing an efficient drive spectrum absent of M-band X-rays using the two-dimensional lagrangian radiation hydrodynamics code h2d. The removal of the M-band transitions is observed in the Cu-lined hohlraum reducing the total X-ray energy above 1.8 keV to 58% that of the un-lined hohlraum. Total radiation energy in the Cu-lined hohlraum is 93% that of the energy in the pure Au hohlraum for a 1 ns pulse. However, the soft X-ray drive energy (below 1.8 keV) for the lined hohlraum is 98% that of the pure Au hohlraum.

INTRODUCTION

Indirect-drive is an inertial confinement fusion (ICF) scheme that utilizes an intermediary known as a hohlraum to convert incident laser energy into X-rays which then drive the implosion of a fuel capsule [2]. Hohlraums are traditionally made from elements with high atomic numbers such as Au due to the approximately linear dependence of laser to X-ray conversion efficiency on proton number Z [3] and their high albedo at high temperatures.

Conversion of laser energy into X-rays takes place in 'hot-spots' which form on the hohlraum wall where the laser energy is absorbed via inverse-bremsstrahlung. X-rays with energy greater than 1.8 keV have been found to have a significant detrimental effect on capsule implosion performance [4] [5]. For high-Z elements such as Au, hard X-rays (> 1.8 keV) generated due to M-band transitions [6], (n = 4 → 3), in these hotspots contribute to capsule preheat and are a source of drive asymmetry on the capsule [1]. It is necessary to dope the ablator with mid-Z to high-Z elements such as Cu, Ge or W in order to attenuate these hard X-rays before they preheat the fuel [7].

Inclusion of dopants in the ablator can be detrimental to implosion performance, increasing the opportunity for Rayleigh-Taylor (RT) growth [8] by introducing more material interfaces thus increasing the number of areas where RT instabilities can develop. The distribution of the dopant therefore is required to be carefully tuned in order to achieve a stable in-flight density gradient at the interfaces. A doped ablator also has a higher mass for a given capsule radius thereby increasing the energy required to reach a given implosion velocity. The presence of high-Z dopant elements leads to increased bremsstrahlung losses from the fuel at stagnation due to 3-D effects that cause ablator-fuel mixing [9].

It has been suggested by R. Olson *et al* that the use of a mid-Z wall liner could lead to a reduction in the higher energy portion of the X-ray drive spectrum, removing the requirement to dope the ablator [10]. Mid-Z liners have also briefly been investigated on the NIF and found to reduce the hard X-ray content of hohlraums by a factor of 2 [11]. In addition, metal foams of zinc have been experimentally shown to reduce the hard X-ray content of hohlraums by a factor of 3 and reduce laser-plasma instabilities [12].

The aim of lining the hohlraum wall with an element such as Cu is to remove the issues associated with a high-Z hohlraum spectrum and improve capsule hydrodynamic performance at the expense of laser conversion efficiency. Tailoring the spectrum, as it has been put, may allow for more robust capsule designs with higher yield-over-clean and a reduction in instability growth.

To understand the effect of lining a hohlraum with a material such as Cu it is important to consider the process by which the laser light is converted into X-rays. The conversion of laser energy into X-rays in a solid target by a nanosecond beam can be understood by considering three distinct zones that form in the target after the laser has begun being absorbed. This approach is studied in more detail by Sigel *et al* in [13] and [14]. Laser energy is absorbed via inverse bremsstrahlung in a low-density conversion layer at the surface of the hohlraum wall called the conversion zone. X-rays produced there are emitted and travel as a diffusive radiation wave, known as a Marshak wave [25], into the optically thick wall (re-emission zone) and are re-emitted with a flux of approximately σT^4 where T is the electron temperature of the wall. The final zone is the comparatively cold shocked material of the high-Z wall. This process is summarised in Figure 1 for the case of a lined hohlraum with the position of the Marshak wave indicated along with a 1-D radial plot of density and radiation temperature in the laser hotspot.

In addition to their efficient conversion of laser en-

* jmo510@york.ac.uk

FIG. 1: Left: Diagram showing a quarter slice of a lined hohlraum depicting the position of the Marshak wavefront, the expanding laser hotspot plasma and the critical-density surface of the laser. Time has passed such that the Marshak wave has propagated into the Au wall and the critical surface remains in the Cu-liner.
Right: A slice through the hohlraum showing the mass density and radiation temperature with regions and the Marshak wave labelled.

ergy into X-rays, high-Z materials are used to form the hohlraum due to their high albedo to thermal X-rays at temperatures of interest, which enables the efficient creation of a high temperature radiation field. Lower-Z elements like Cu have a lower albedo than high-Z elements such as Au. This combined with the lower X-ray conversion efficiency means that a pure Cu hohlraum achieves a lower radiation temperature than an equivalent Au hohlraum.

A Cu-lined Au hohlraum on the other hand should be able to convert laser energy into X-rays in the Cu layer while maintaining a high X-ray opacity in the Au re-emmission layer and therefore a higher radiation temperature than a pure Cu hohlraum.

The electron temperature in the conversion layer (laser hotspots) is several keV, high enough to efficiently pump M-band transitions in Au. Cu hotspots, however, would be dominated by L-shell emission below 1.8 keV at relevant temperatures. Therefore Cu as a conversion medium should be superior with regards to producing a drive spectrum with fewer higher energy X-rays.

It is important to note that lining a hohlraum with a mid-Z element is a different situation to creating a 'cocktail' hohlraum where the opacity of the hohlraum is increased by mixing materials with complimentary opacity structures in the wall, though it is true that doing this may also result in a reduction in M-band X-rays. Depleted uranium has for instance been used extensively interleaved with gold [26]. This not only increases the opacity of the wall to the thermal X-rays within the body of the hohlraum but also reduces the fraction of radiation energy at higher energies due to the fact that the M-band of uranium is more difficult to excite, lying as it does at a somewhat higher energy than in Au [15][16].

However, shifting the M-band to higher energies in order to suppress it can also have a downside. Fast-fission, a reaction that underpins the operation of fast-breeder reactors [17], can occur in cocktail hohlraums containing depleted Uranium, driven by the MeV neutrons produced in the fusion of deuterium and tritium. The presence of uranium and its fission products in the reactor vessel complicates operations and handling requirements and also impacts upon some of the key benefits of fusion as a 'clean' energy source.

The approach of employing a mid-Z liner is to reduce the M-band by using an element with a comparatively low atomic number as the interface with the laser. So, rather than increasing the energy needed to excite M-band transitions, the availability of such transitions is removed altogether in the surface material.

While the near-term focus of the ICF programme remains squarely upon ignition, mid-Z wall liners will only be of interest if the losses incurred by the reduced conversion efficiency are outweighed by the performance of an un-doped capsule. In this work the performance of an un-doped capsule is not studied, however implosions at the NIF have shown that capsules with reduced dopant amounts driven by a depleted-uranium (DU)-Au hohlraum can result in higher stagnation pressures and improved neutron yield [29]. The reduction in dopant concentration benefits the implosion performance in ways previously stated and is facilitated by the reduction in M-band radiation due to the DU-Au hohlraum. It was also found that dopants increase the albedo of the ablator due to re-radiation of the incident X-rays by the dopant atoms, thus reducing the ablation pressure at the capsule surface. Using an ablator with reduced dopant concentration can result in a higher drive pressure and a lower ablator mass, therefore perhaps offsetting losses incurred by the use of Cu as the conversion medium for the laser energy.

In addition, it is important to note subtleties in interpreting the conversion efficiency of the laser into X-rays for a high-Z hohlraum and for a mid-Z hohlraum. While the conversion of incident laser energy into total X-ray energy for a high-Z hohlraum may be higher than for a mid-Z hohlraum, the fraction of the incident laser energy that is converted into X-rays with energy above 1.8 keV is also higher. These higher energy X-rays are unwanted and negatively affect the performance of the capsule implosion. Therefore the conversion efficiency of laser light into soft X-rays (< 1.8 keV) is a better measure of the laser-hohlraum coupling and one that may allow the pros and cons of using a mid-Z liner to be more accurately assessed.

In this study the ability of a mid-Z lined hohlraum to produce radiation temperatures comparable to an unlined gold hohlraum and to reduce hard X-ray spectral content is investigated using the radiation hydrodynamics code, h2d [18].

H2D PHYSICS DESCRIPTION

The radiation transport used in h2d is a multi-group diffusive model that is accurate for optically thick plasmas, which in our case corresponds to the high density blow-off plasma in the re-emission region. This approximation holds for the majority of the hohlraum with the exception of radiation transport within the optically thin blow-off plasma of the hotspot conversion region. Diffusive transport tends to artificially increase the isotropy of the radiation drive. However the effect of non-uniformity in the radiation field is not critical to the assessments being made in this paper, which concern hohlraum energetics and the available drive spectrum.

The radiation energy contained within the hohlraum is generated in the laser hotspots and so it is important to accurately model both the laser deposition and the atomic physics that occurs there. The laser energy is deposited via inverse bremsstrahlung with the coefficient of absorption obtained from the collisional model being used, here Spitzer-Harm [19]. Equilibration then occurs via collisions between the electrons and the ion species and the plasma undergoes expansion.

The process of modelling the atomic physics occurring within the laser hotspot involves several assumptions regarding the equilibrium between the radiation and the plasma. H2d can solve the individual rate equations for excitation and de-excitation of bound electrons in a time-dependant manner allowing the assumption of local thermodynamic equilibrium (LTE) to be relaxed, thus better approximating the plasma in the optically thin laser hotspot region and the mid-Z liner.

The bulk of the hohlraum wall, where the Marshak wave travels, has a short optical mean-free-path and the dynamics are determined by the ablation of the plasma as the X-rays diffuse into the wall. For a high opacity wall this situation can be modelled using an LTE model. The laser hotspot, however, requires a non-LTE treatment due to its low opacity to the X-rays it generates. In addition, the non-local heat flux due to high energy electrons generated through laser absorption processes further complicate modelling of the laser hotspot. In h2d the effects of non-local transport are mimicked by adjusting the flux-limiter in the diffusion model for electron conduction. The value of the flux-limiter employed in a given simulation is usually adjusted to fit experimental results. Experiments on the NIF have been modelled using a range of flux-limiter values from 3% to 15% of the free-streaming limit [20]. Since the present study is entirely simulation-based, and in order to maintain consistency between the Cu-lined and pure Au hohlraum cases, the same value of 10% is used for both cases. Equation of state information is provided by SESAME tables and opacities are calculated in-line by h2d's screened-hydrogenic atomic physics package which solves the time dependant rate equations for non-LTE. A $\times 1.4$ opacity multiplier has been applied to the gold region in order to bring the calculated temperatures in line with scaling laws that are based on experimentally determined albedos [21].

The results collated by Ren *et al* [21] have been used to benchmark h2d. The design of the hohlraum is similar to those used in [22]. H2d has been found to produce temperatures in the range of experimental and simulated hohlraums of similar design.

FIG. 2: To the left of the divide in the diagram the dimensions of the hohlraum used in this work are shown. The right side shows the arrangement of the lasers into the inner and outer rings. The Z axis is an axis of symmetry.

PROBLEM DESCRIPTION

The hohlraums modelled are cylindrical in shape and of length 10.1 mm and diameter 5.75 mm (see figure 2). There is a laser entrance hole at both ends of the cylinder of diameter 3.37 mm. For simplicity there is no window material used in the laser entrance holes, the laser beams enter and are incident on the hohlraum from the onset of the pulse. Beams are arranged as shown in figure 2 into an inner and outer ring comprised of 8 and 16 cones respectively which enter the hohlraum from both sides and illuminate the inner surface in two sets of two rings. Here the laser intensity is calculated in-line by h2d utilizing a 3-D ray tracing package which decomposes the 3-D laser arrangement into the 2-D simulation space used to model the hohlraum. Here a cylindrical (R-theta) geometry is used with a mesh zone resolution of < 1 nm feathered in the direction of the laser interaction surface. Laser power is delivered in a 1 ns square pulse with a 0.5 ns rise and a peak power of 250 TW. At the peak power of the pulse the laser irradiance for the outer and inner set of beams is $8{\times}10^{14}$ W cm^{-2} and $3.5{\times}10^{14}$ W cm^{-2} respectively. To model the radiation 150 groups were used, logarithmically spaced up to a photon energy of 20 keV with the high-energy region between 1.8 keV - 6 keV containing 20 groups.

Two hohlraums have been investigated, one with a 25 μm thick Au wall, the other a 25 μm Au wall with a 0.5 μm Cu layer covering the entire inner surface. Both hohlraums contain a gas fill of helium at a density of 0.1 mg/cc to tamp wall motion.

FIG. 3: The radiation temperature inside the hohlraum as a function of time calculated by running h2d with a NLTE atomic physics model. The laser pulse profile is inset. The lined hohlraum is given in grey and the Au hohlraum is given in black.

FIG. 4: The total radiation energy density inside the hohlraum (solid) is plotted along with the total radiation energy contained in the X-rays having energy below 1.8 keV (dashed). The fraction of the total radiation energy in the hard X-rays (> 1.8 keV) as a function of time is inset. The lined hohlraum is given in grey and the Au hohlraum in black.

RESULTS

Results from the radiation hydrodynamics simulations show that the Cu-lined Au hohlraum produces a lower radiation temperature than the pure Au hohlraum for the majority of the pulse (figure 3). Lining the inside surface of the hohlraum with a layer of Cu results in a greater energy loss due to the hydrodynamic motion of the liner as it is ablated by the lasers and the radiation field.

Towards the end of the pulse the radiation temperature in the Cu-lined hohlraum approaches that of the Au hohlraum. The Au hohlraum peaks at a radiation temperature of 274 eV while the Cu-lined Au hohlraum peaks at 272 eV. The slower rise can be attributed to the greater energy loss due to the expansion of the Cu liner and lower conversion efficiency into X-rays in the Cu liner material. As the liner becomes more optically thin to the X-rays the energy loss due to liner heating and expansion decreases.

The radiation energy density in the hohlraum as a function of time is plotted in figure 4, and shows the evolution of the total X-ray energy alongside the soft X-ray (< 1.8 keV) energy for the pure Au and Cu-lined hohlraum. Total energy in the hard X-rays (> 1.8 keV) in the Cu-lined hohlraum is 58% of that contained in the pure Au hohlraum and remains lower for the duration of the pulse, including the initial peak. The total radiation energy in the Cu-lined hohlraum is lower than in the pure Au hohlraum but a significant portion of the energy in the Au hohlraum is contained in the hard X-ray component which is effectively working against the efficient implosion of the capsule through introduction of drive asymmetry and preheating. When comparing the dashed lines in figure 4 we see that the energy below 1.8 keV for the Cu-lined hohlraum is 98% that of the pure Au hohlraum. Since the X-rays above 1.8 keV are detrimental to implosion performance this measure is more indicative of the effectiveness of the Cu liner.

The pulse used here is 1 ns which is short compared to a normal indirect-drive ignition pulse of around 15 ns and so the present study merely confirms the ability of a mid-Z lined hohlraum to produce radiation temperatures similar to that of an un-lined gold hohlraum in this particular scenario. Studying the use of a liner over a longer time period is challenging using h2d due to material convergence on the hohlraum axis and the requirement to effectively deal with very large deformations in the lagrangian mesh.

After enough of the liner has become optically thin and the Marshak wave has propagated into the Au layer the radiation temperature in the Cu-lined holraum approaches that of the pure Au hohlraum. Line-outs in figure 6, taken at z = 0.28 cm (centre of hotspot bubble) at a time of 1.0 ns from the start of the pulse, show the plasma density and electron temperature as a function of radial position. Three distinct regions can be identified, the low-density and high-temperature conversion region at the front of the expanding plasma, beyond that the optically thick re-emission region and finally the colder wall material ahead of the Marshak wave. The thin layer of Cu has little impact on the Marshak wave as it is less opaque to the X-rays than the Au material that makes up the bulk of the wall. In areas where only the X-rays are incident the Au hohlraum re-emission region is less expanded than that of the the Cu-lined Au due to the higher ablation velocity of the Cu liner. This is due to the higher sound speed in Cu than in Au which can be used as an estimate for the relative expansion velocities [24]. In areas where the laser is incident the ablation of the wall due to the laser causes the critical surface of the laser to move into the wall. This results in a thinner re-emission region for both lined and un-lined hohlraums in these areas as can be seen in figure 5.

In the laser hotspot conversion region the Cu-lined hohlraum has expanded further and is of a higher density than in the Au hohlraum. For longer pulses the laser bubble will undergo more expansion in the case of a lined hohlraum and will grow to impede the inner beam propagation earlier in the pulse than for a pure Au hohlraum, since the ratio of expansion speeds v_{cu}/v_{au} can be estimated with the ratio of ion masses, $\sqrt{m_{au}/m_{cu}} \approx 3$ [24]. The lower Z of Cu will mean that less energy will be lost from the pulse due to inverse bremsstrahlung in the low-density Cu plasma. However, the impact of cross-beam energy transfer [27] due to this increased Cu fill earlier in the pulse remains to be determined for a pulse of length similar to those used on the NIF with the aim of achieving ignition.

An important point to consider is whether the benefit of a Cu liner is retained as we increase the thickness of the liner. The more time spent traversing the liner by the Marshak wave the more energy is lost to heating the lower albedo Cu, resulting in a lower hohlraum temper-

FIG. 5: NLTE two-dimensional mass density plot of the Cu-lined Au hohlraum (left) and the Au hohlraum (right) at t = 1.0 ns . Motion of the wall in the lined hohlraum is greater than that of the un-lined hohlraum due to the lower mass of the liner and similar radiation temperatures generated in both hohlraums. The laser hotspot region in the lined hohlraum is also further expanded for the same reason but does not impede laser propagation for the pulse length considered. Material boundaries are marked with solid black lines.

FIG. 6: Density (solid) and electron temperature (dashed) lineouts of the laser hotspot generated by the outer set of beams at 1.0 ns. Three distinct regions can be identified from left to right in the figure (as indicated by the shaded regions); the low-density and high-temperature region at the front face of the wall, the optically thick re-emission region beyond that and the high density colder wall material which extends back to the shock front. The vertical blue line indicates the Cu-Au material boundary in the lined hohlraum case.

FIG. 7: Plots of the X-ray flux at the hohlraum axis for the total X-ray flux (solid line) and the $>$ 1.8 keV X-ray flux (dashed line), each normalized respectively. The flux profiles at two times are given: (grey) 0.25 ns, before the marshak wave enters the gold; (black) 0.5 ns, after the Marshak wave has crossed into the gold.

ature when compared to a pure Au hohlraum. The determining factors are the time taken for the laser to burn through the liner, such that the critical surface of the laser has entered the Au, and the speed of the Marshak wave in the liner. The first factor leads to the minimum thickness, d_l needed for a liner of a given density being irradiated by a laser with a certain mass ablation rate in order that no direct laser heating of the Au occurs.

$$\rho_l d_l \geq \int_0^\tau \dot{m}_a dt \tag{1}$$

where $\dot{m}_a$ is the mass ablation rate in units of g cm^{-2}s^{-1}, τ is the pulse length in seconds and ρ_l is the density of the liner.

For the Au backing to play a role in the radiation confinement the time taken by the Marshak wave to traverse the liner should be small, such that

$$\frac{d_l}{v_M} << \tau \tag{2}$$

where d_l is the thickness of the liner, v_M is the Marshak wave velocity, which depends inversely on the material opacity [25], and τ is the laser pulse length.

Figure 5 shows the hohlraum towards the end of the laser pulse (t = 1.3 ns). The difference in wall expansion between the lined and un-lined hohlraum can be seen as well as the increased expansion of the laser hotspot region in the Cu-lined hohlraum due to the Cu liner's lower density. Due to the short duration of this pulse there is not yet sufficient hohlraum wall motion to impede laser transport to the hotspot.

Additionally, figure 7 shows the X-ray flux profile on the hohlraum axis both before and after the Marshak wave has propagated into the gold for both the total X-ray flux and the hard X-ray flux (>1.8 keV). It can be seen that the total flux asymmetry is reduced in the Cu-lined hohlraum due to the reduction in the hard X-rays which exclusively originate in the laser hotspot regions of the hohlraum. Once the Marshak wave has propagated into the gold in the lined hohlraum the deviation on axis of the hard X-ray flux from uniformity is around 2.5% whereas for the un-lined hohlraum at the same time it is 10%. While these simulations were not designed to study the drive symmetry, and so are not optimised as such, the results still show a potential benefit of reducing the hard X-ray content of the drive spectrum with respect to improving capsule implosion symmetry.

CONCLUSION

Cu-lined Au hohlraums have been shown to suppress the generation of harder X-rays ($>$ 1.8 keV) and produce 98% the soft X-ray energy ($<$ 1.8 keV) of an equivalent un-lined Au hohlraum. The total energy contained in the X-rays with energy above 1.8 keV is reduced to 58% of unlined-Au levels when lining the hohlraum with 0.5 μm of Cu and remains at low levels throughout the pulse.

Further work is required in order to extend the application of liners to longer pulses designed for capsule implosions. For longer pulses, measures may need to be taken to avoid excessive hohlraum fill that could affect deposition of laser energy, particularly with the inner set of beams that could suffer from cross-beam-energy-transfer early in the pulse [27]. Novel hohlraum designs that aim to reduce laser hotspot motion [28] could be applied to mid-Z liners in order to counteract the increased wall motion that results from the lower-density liner. Also, the liner heating losses could be mitigated further by selectively lining only the surface of the hohlraum where the lasers are incident, thus allowing the X-rays to be incident on the high albedo Au rather than to having to first burn through the layer of Cu.

Future work will involve simulations of un-doped and reduced-dopant capsules in order to better understand the effect of the drive produced by Cu-lined hohlraums on the implosion efficiency. Previous work by Dewald *et al* [29] has shown that un-doped capsules driven by a spectrum with reduced M-band, achieved in this case via utilising a depleted-uranium hohlraum, results in increased gain over doped capsules by increasing the hydrodynamic performance of the capsule and by reducing radiative effects introduced by the ablator dopant. It may be true that these effects conspire to produce an increase in overall efficiency of the hohlraum-capsule target for a Cu-lined hohlraum despite the weaker X-ray drive but longer, shaped pulses designed to compress and ignite a fuel capsule will need to be studied in order to quantify this effect.

ACKNOWLEDGEMENTS

The authors would like to thank R. Trines and R. Scott and the Rutherford Appleton Laboratory for providing access to and maintaining the computing systems on which h2d was used. This work was supported by the Engineering and Physical Sciences Research Council [EP/L01663X/1].

DATA AVAILABILITY

Data is available upon reasonable request from the authors.

[1] Y. Li, J. Gu, C. Wu, P. Song, Z. Dai, S. Li, Physics of Plasmas 23, 7, 072705 (2016)
[2] J. Lindl, Physics of Plasmas 2, 11, 3933-4024 (1995)
[3] M. Murakami, and J. Meyer-ter-Vehn, Nuclear Fusion 31, 7, 1315-1331 (1991)
[4] J. Gu, , S. Zou, , Y. Li , Z. Dai, W. Ye, Phys. Plasmas 19, 122710 (2012).
[5] R. E. Olson, R. J. Leeper, A. Nobile, J. A. Oertel, Phys. Rev. Lett. 91, 235002, (2003).
[6] H. F. Robey, T. S. Perry, H. S. Park, P. Amendt, C. M. Sorce, S. M. Compton, K. M. Campbell, J. P. Knauer, Phys. Plasmas 12, 1–7 (2005).
[7] S. W. Haan, M. C. Herrmann, T. R. Dittrich, A. J. Fetterman, M. M. Marinak, D. H. Munro, S. M. Pollaine, J. D. Salmonson, G. L. Strobel, L. J. Suter, Physics of Plasmas 12, 5, 056316 (2005)
[8] R. Betti, V. N. Goncharov, R. L. McCrory, C. P. Verdon, Phys. Plasmas 5, 1446 (1998).
[9] D. S. Clark, M. M. Marinak, C. R. Weber, D. C. Eder, S. W. Haan, B. A. Hammel, D. E. Hinkel, O. S. Jones, J. L. Milovich, P. K. Patel, *et al*, Phys. Plasmas 22, 022703 (2015).
[10] R. E. Olson, G. A Rochau, E. L. Dewald, J. L. Kaae, R. J. Leeper, and L. J Suter, *Modification of a laser Hohlraum spectrum via a Mid-Z Wall Liner* , Bulletin of the American Physical Society, Program of the 46th Annual Meeting of the Division of Plasma Physics (2004)
[11] J. D. Moody, D. A. Calahan, D. E. Hinkel, P. A. Amendt, K. L. Baker, D. Bradley, P. M. Celliers, E. L. Dewald, L. Divol, T. Döppner, Physics of Plasmas 21, 056317, (2014)
[12] P. Fitzsimmons, F. Elsner, R. Paguio, A. Nikroo, C. Thomas, K. Baker, H. Huang, M. Schoff, D. Kaczala, H. Reynolds *et al*, Fusion Science and Technology 73, 210–218, (2018)
[13] R. Sigel, K. Eidmann, F. Lavarenne, R. F. Schmalz, Physics of Fluids B: Plasma Physics 2, 199 (1990)
[14] K. Eidmann, R. F. Schmalz, R. Sigel, Physics of Fluids B: Plasma Physics 2, 208 (1990)
[15] H. L.Wilkens, A. Nikroo, D. R. Wall, J. R Wall, Physics of Plasmas 14, 056310 (2007).
[16] L. Guo, Y. Ding, P. Xing, S. Li, L. Kuang, Z. Li, T. Yi, G. Ren, Z. Wu, L. Jing, *et al*, New J. Phys. 17, 11 (2015).
[17] T. B. Cochran, . A. Feiveson, W. Patterson, G. Pshakin, M. V. Ramana, M. Schneider, T. Suzuki, F. von Hippel, *Fast Breeder Reactor Programs: History and Status*, International Panel on Fissile Materials (2010)
[18] J. T. Larsen and S. M. Lane, Journal of Quantitative Spectroscopy and Radiative Transfer 51, 1–2, p. 179-186, (1994)
[19] R. S. Cohen, L. Spitzer, P. Routly, Physical Review 80, 2 (1950)
[20] O. S. Jones, L. J. Suter, H. A. Scott, M. A. Barrios, W. A. Farmer, S. B. Hansen, D. A. Liedahl, C. W. Mauche, A. S. Moore, M. D. Rosen, *et al*, Phys. Plasmas 24, 056312 (2017).
[21] G. Ren, J. Liu, , W. Huo, K. Lan, Matter Radiat. Extrem. 2, 22–27 (2017).
[22] L. F. Berzak Hopkins, S. Le Pape, L. Divol, N. B. Meezan, A. J. Mackinnon, D. D. Ho, O. S. Jones, S. Khan, J. L. Milovich, J. S. Ross, *et al*, Phys. Plasmas 22, 056318 (2015)
[23] T. R. Dittrich, O. A. Hurricane, D. A. Callahan, E. L. Dewald, T. Döppner, D. E. Hinkel, L. F. Berzak Hopkins, S. Le Pape, T. Ma, J. L. Milovich, *et al*, Physical Review Letters, 112 (2014)
[24] J. E. Ralph, O. Landen, L. Divol, A. Pak, T. Ma, D. A. Callahan, A. L. Kritcher, T. Doppner, D. E. Hinkel, C. Jarrot *et al*, Physics of Plasmas 25, 082701 (2018)
[25] R. E. Marshak, Phys. Fluids 1, 24 (1958)
[26] T. Doppner, D. A. Callahan, O. A. Hurricane, D. E. Hinkel, T. Ma, H.-S. Park, L. F. Berzak Hopkins, D. T. Casey, P. Celliers, E. L. Dewald, *et al*, Phys. Rev. Lett. 115, 055001 (2015)
[27] W. L. Kruer, S. C. Wilks, B. B. Afeyan, R. K. Kirkwood, Physics of Plasmas 3, 382 (1996)
[28] M. Vandenboomgaerde, A. Grisollet, M. Bonnefille, J. Clérouin, P. Arnault, N. Desbiens, L. Videau, Phys. Plasmas 25, 1, 012713 (2018).
[29] E. L. Dewald, R. Tommasini, N. B. Meezan, O. L. Landen, S. Khan, R. Rygg, J. Field, A. S. Moore, D. Sayre, A. J. MacKinnon, *et al*, Phys. Plasmas 25, 092702 (2018).

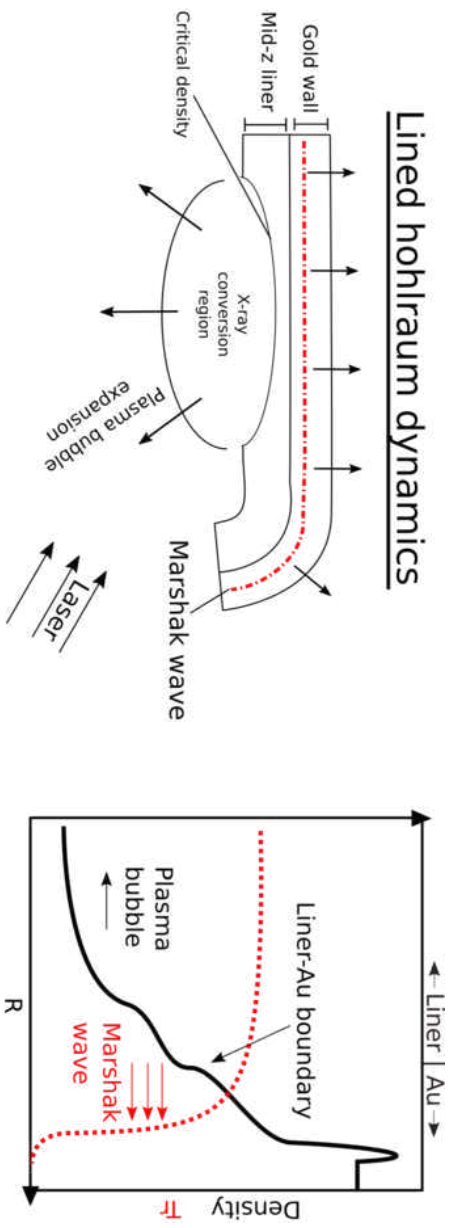

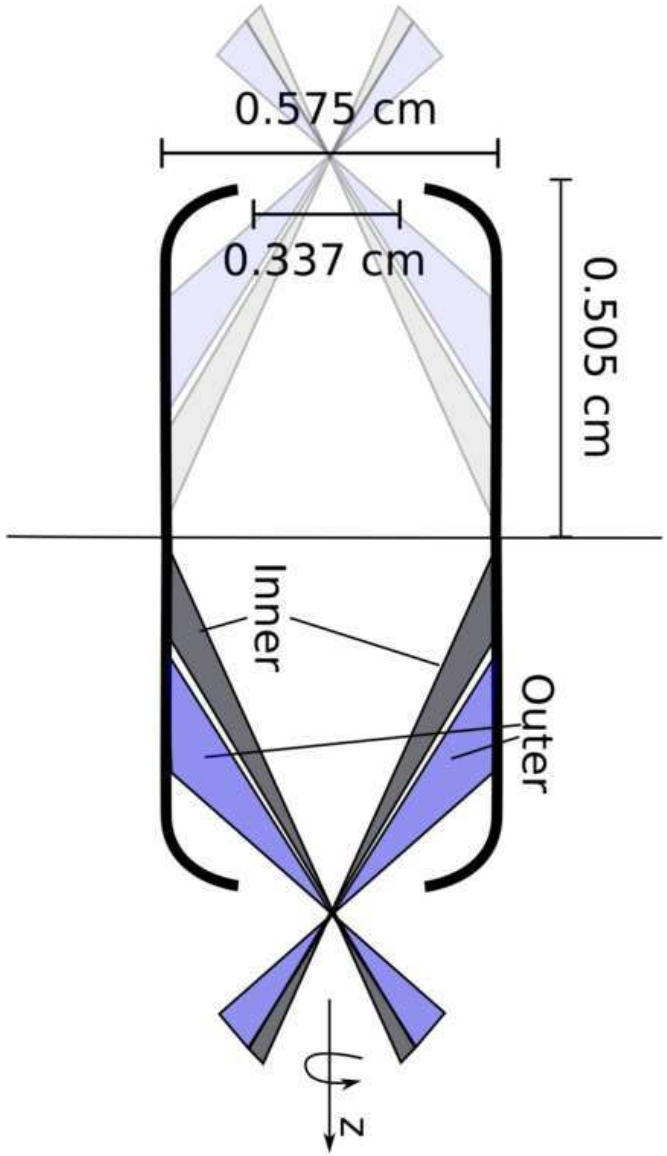

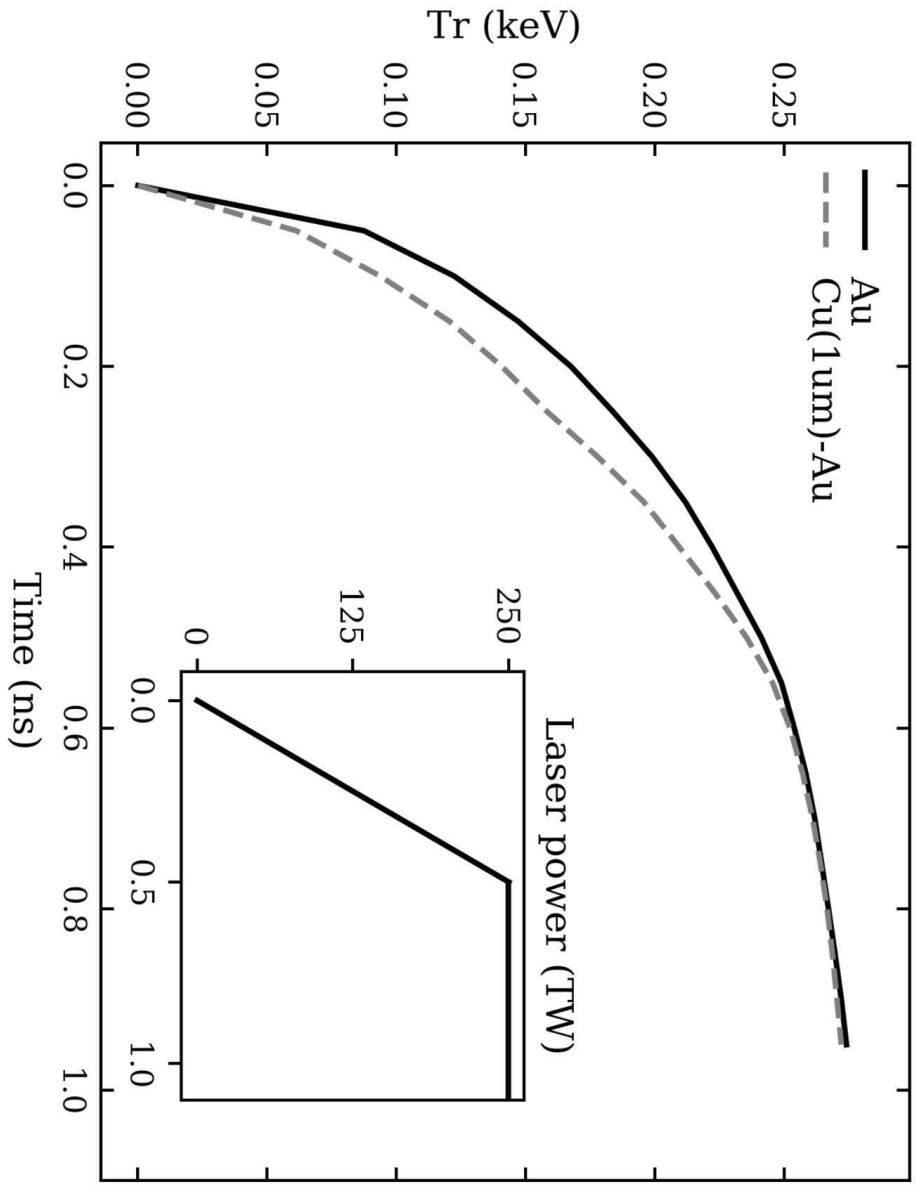

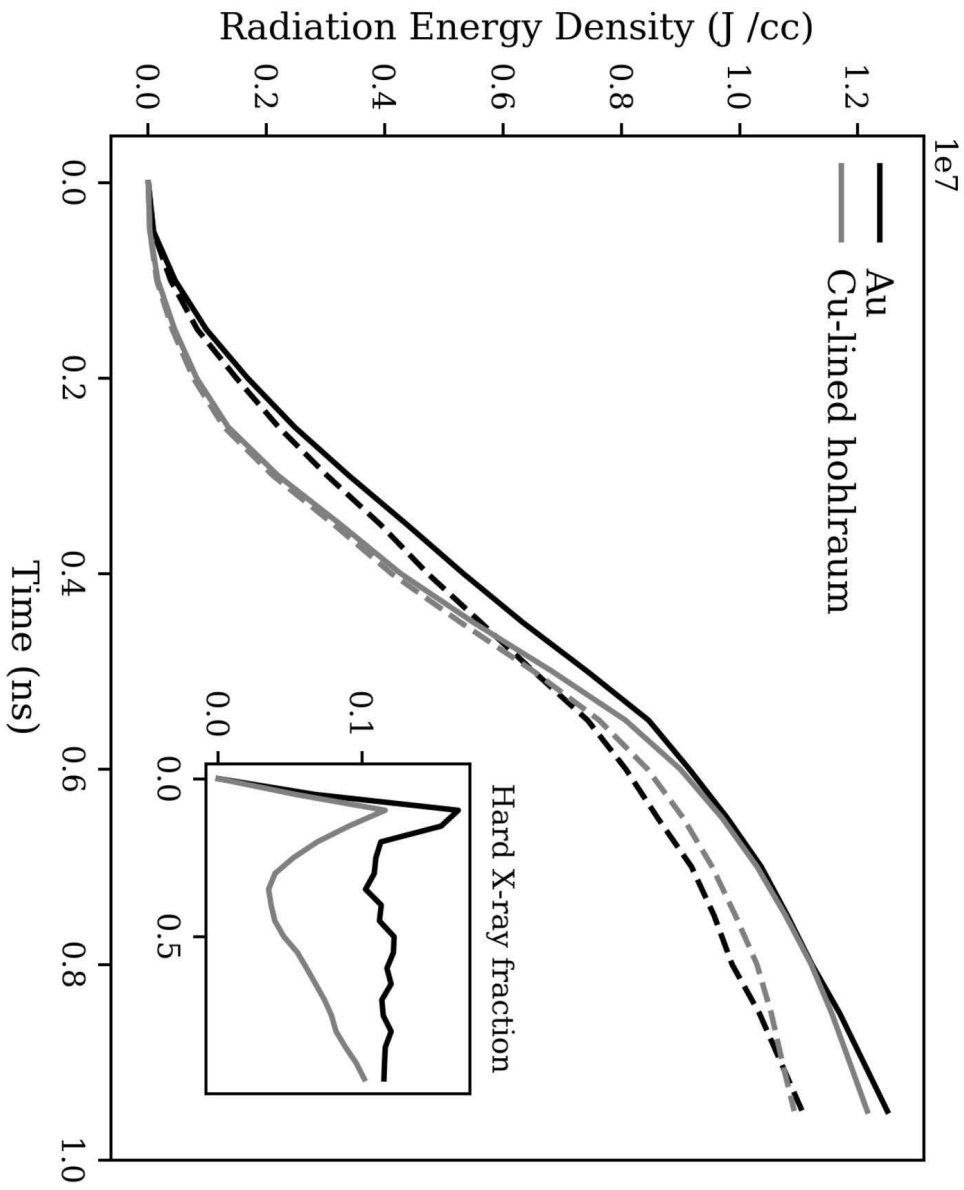

PLEASE CITE THIS ARTICLE AS DOI: 10.1063/5.0029689